

Broad absorption line symbiotic stars: highly ionized species in the fast outflow from MWC 560

Adrian B. Lucy,^{1*†} Christian Knigge,² and J. L. Sokoloski¹

¹*Columbia University, Dept. of Astronomy, 550 West 120th Street, New York, NY 10027, U.S.A.*

²*University of Southampton, School of Physics & Astronomy, Highfield, Southampton, SO17 1BJ, U.K.*

ABSTRACT

In symbiotic binaries, jets and disk winds may be integral to the physics of accretion onto white dwarfs from cool giants. The persistent outflow from symbiotic star MWC 560 (\equiv V694 Mon) is known to manifest as broad absorption lines (BALs), most prominently at the Balmer transitions. We report the detection of high-ionization BALs from C IV, Si IV, N V, and He II in *International Ultraviolet Explorer* spectra obtained on 1990 April 29–30, when an optical outburst temporarily erased the obscuring ‘iron curtain’ of absorption troughs from Fe II and similar ions. The C IV and Si IV BALs reached maximum radial velocities at least 1000 km s⁻¹ higher than contemporaneous Mg II and He II BALs; the same behaviors occur in the winds of quasars and cataclysmic variables. An iron curtain lifts to unveil high-ionization BALs during the P Cygni phase observed in some novae, suggesting by analogy a temporary switch in MWC 560 from persistent outflow to discrete mass ejection. At least three more symbiotic stars exhibit broad absorption with blue edges faster than 1500 km s⁻¹; high-ionization BALs have been reported in AS 304 (\equiv V4018 Sgr), while transient Balmer BALs have been reported in Z And and CH Cyg. These BAL-producing fast outflows can have wider opening angles than has been previously supposed. BAL symbiotics are short-timescale laboratories for their giga-scale analogs, broad absorption line quasars (BALQSOs), which display a similarly wide range of ionization states in their winds.

Key words: binaries: symbiotic — stars: winds, outflows — accretion, accretion discs — quasars: absorption lines — stars: individual: MWC 560, AS 304

1 INTRODUCTION

Accretion onto compact objects exhibits similar phenomenology across a wide range of mass scales, spanning over nine orders of magnitude from supermassive black holes to white dwarfs. In fact, MWC 560 (\equiv V694 Mon) and CH Cyg—each believed to constitute a white dwarf (WD) accreting from a red giant (RG), the most common kind of symbiotic star—have been called ‘nano-quasars,’ because broadening their emission lines by a factor of 10 produces optical spectra that almost identically resemble the archetypal Seyfert 1 galaxy I Zw 1 (Zamanov & Marziani 2002).

MWC 560 also usually exhibits blue-shifted broad absorption lines (BALs¹) from a jet (Schmid et al. 2001) or disk wind. The blue edges of these lines vary between

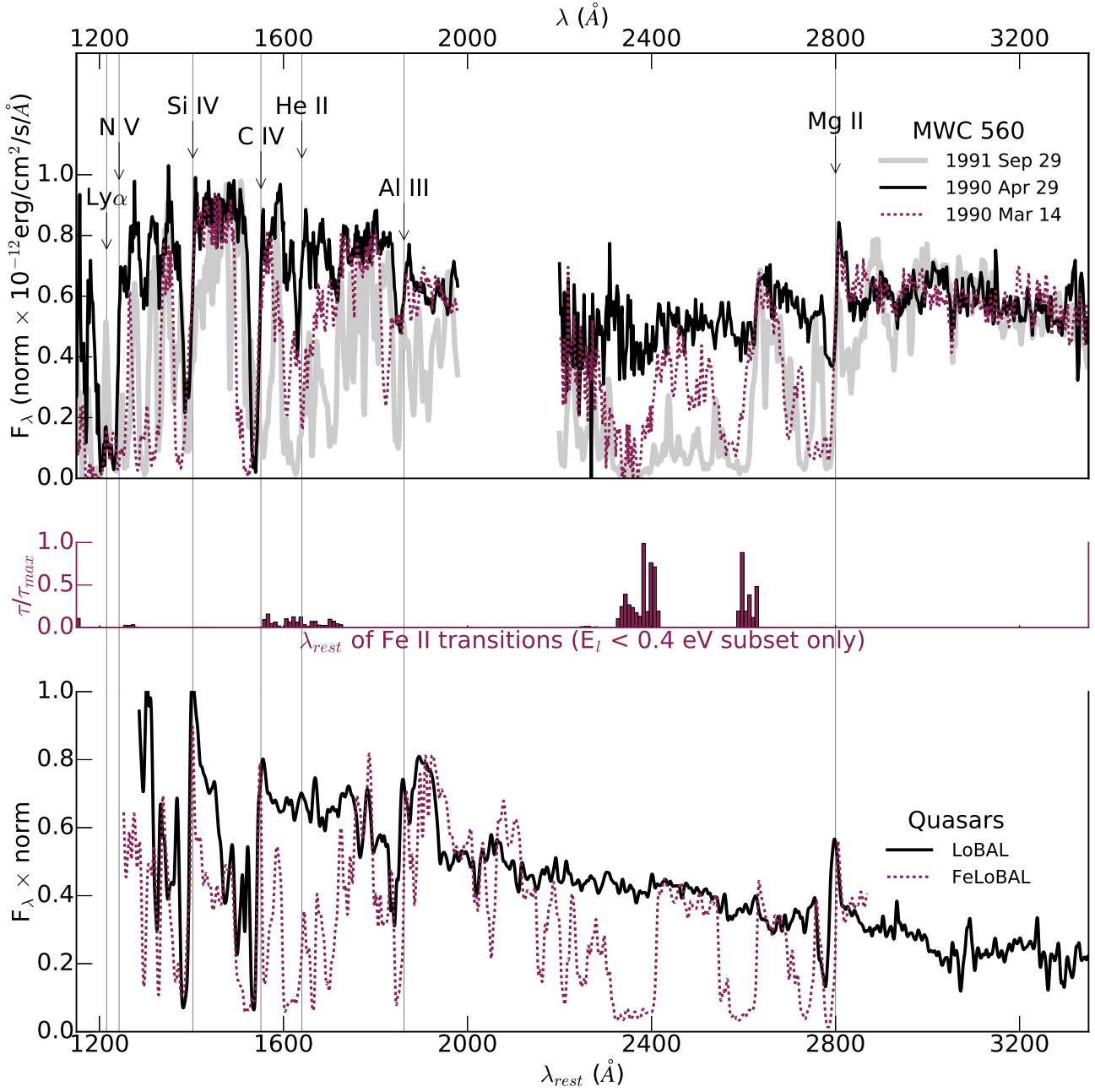
900–6000 km s⁻¹ from the Balmer transitions and combinations of Al III, Mg II, Fe II, Cr II, Si II, C II, Ca II, Mg I, Na I, O I, and He I, including various excited-state, metastable-state, and resonance transitions (Tomov et al. 1990a, 1992; Michalitsianos et al. 1991; Schmid et al. 2001; Meier et al. 1996). MWC 560 thus resembles the rare subset of Fe II low-ionization BAL quasars (FeLoBALs) with Balmer BALs; symbiotic nebulae typically have electron densities up to 10⁸–10¹² cm⁻³, comparable to the densities necessary to populate Balmer absorption in photo-ionized quasar winds (Hall 2007; Leighly et al. 2011; Williams et al. 2017). However, MWC 560 has seemed to be missing the set of higher-ionization ultraviolet (UV) resonance BALs—C IV λ 1550Å, Si IV λ 1400Å, and N V λ 1240Å—exhibited by many cataclysmic variable (CV) winds (Shlosman & Vitello 1993) and all BAL quasars outflows (Weymann et al. 1991).

Optical flickering from the accretion disk, TiO bands from the M giant, and BALs from the disk outflow led Bond et al. (1984) to an accurate description of MWC 560, but the system became popular during an optical brightening peak in 1990. The Balmer BALs reacted dramatically,

* lucy@astro.columbia.edu

† LSSSTC Data Science Fellow

¹ We ignore the distinction between BALs and mini-BALs appearing in the quasar context, where the richer sample size sometimes motivates formalism (e.g., Knigge et al. 2008).

**Figure 1.**

Top panel: IUE spectra show that MWC 560’s iron curtain obscured the UV in 1990 March, vanished in 1990 April, and returned by 1991 September. We re-normalized all spectra to the maximum (1990 April 29) median flux density longward of 3000 \AA , and did not deredden. Line identifications for the 1990 April spectrum are marked at their rest wavelengths.

Middle panel: Predicted optical depth (τ) relative to the strongest value (τ_{max}), for the Fe II transitions from near the ground state (§ 3.2) in 10 \AA bins, excluding higher-excitations populated during iron curtain phases (e.g., on the blue wing of Mg II).

Bottom panel: The Balmer FeLoBAL quasar J172341.1+555340.5 (Hall et al. 2002) resembles the iron curtain states of MWC 560, while the LoBAL quasar J140125.6+581650.7 (Gibson et al. 2009) resembles the 1990 April spectrum (§ 4.3). These Sloan Digital Sky Survey spectra were obtained from the Science Archive Server, corrected for redshift and the negligible Galactic extinction on their sightlines (Green et al. 2015), normalized to match pseudo-continua on an arbitrary scale, and smoothed to resolving power $R=400$. The FeLoBAL was further dereddened in its rest frame for $E(B-V)=0.15$ of SMC bar extinction (Gordon et al. 2003).

with blue edges up to 6000 km s^{-1} shifting by thousands of km s^{-1} in mere days (Tomov et al. 1990a), and the inner accretion disk may have been partially evacuated during that year (Zamanov et al. 2011a). MWC 560 later attracted renewed interest in 2016, when it brightened to $V \approx 9$ for the first time since 1990 (Munari et al. 2016). No signs of inner-disk evacuation were observed in 2016—and once the peak optical flux was reached, the Balmer BALs varied stably alongside weeks-long changes in the accretion rate, with blue edges up to 3000 km s^{-1} at most (Lucy et al., in preparation). The 1990 optical high state thus remains a uniquely volatile incident in the recorded history of MWC 560. As we will show, there are still new insights to be gleaned from the 28-year-old observations of this event.

Setting the stage for our analysis, MWC 560’s UV spectrum is usually obscured by a curtain of absorption by Fe II and similar ions (Michalitsianos et al. 1991). This iron curtain weakened dramatically by the end of 1990 April (Skopal 2005), allowing us to see the outflow in a rare, unobscured state. When the next UV spectrum was obtained, on 1990 September 26, the Fe II absorption had returned with even more optical depth than before (Maran et al. 1991). The iron curtain was never again observed to vanish, even during *Swift* observations throughout the 2016 optical high state (Lucy et al., in preparation).

The paper is structured as follows: We describe the archival data (§ 2). We show that a total disruption of the iron curtain in 1990 April unveiled high-ionization UV BALs, which were previously misidentified as Si II and Fe II (§ 3). We discuss the physical consequences of this finding—including connections to quasars and novae—and the disappearance of the iron curtain, which has been optically thick at every other epoch (§ 4.1–§ 4.3). The high-ionization BALs link MWC 560 with symbiotic star AS 304 ($\equiv V4018 \text{ Sgr}$), and show that these objects are prototypes for an emerging class of BAL symbiotics (§ 4.4). Last, we summarize our conclusions (§ 5).

All velocities and wavelengths for MWC 560 are heliocentric.

2 DATA

We retrieved NEWSIPS pipeline reductions of several *International Ultraviolet Explorer* (IUE) large-aperture spectra in the far-UV (FUV; $1150\text{--}1975\text{\AA}$) and near-UV (NUV; $1910\text{--}3300\text{\AA}$), including all UV spectra observed in 1990 April, from the Mikulski Archive for Space Telescopes (MAST). Table 1 lists the spectra, which were previously published in Michalitsianos et al. (1991), Maran et al. (1991), and Bond et al. (1984).

Fig. 1 exemplifies the low-resolution ($4\text{--}8\text{\AA}$) spectra. The chosen dates follow Figure 1 in Skopal (2005), which was designed to exhibit the varying depths of MWC 560’s iron curtain.

3 RESULTS: LINE IDENTIFICATION

3.1 High-ionization BALs

The deepest absorption features in the 1990 April 29.90 and 30.02 spectra are located at the expected pos-

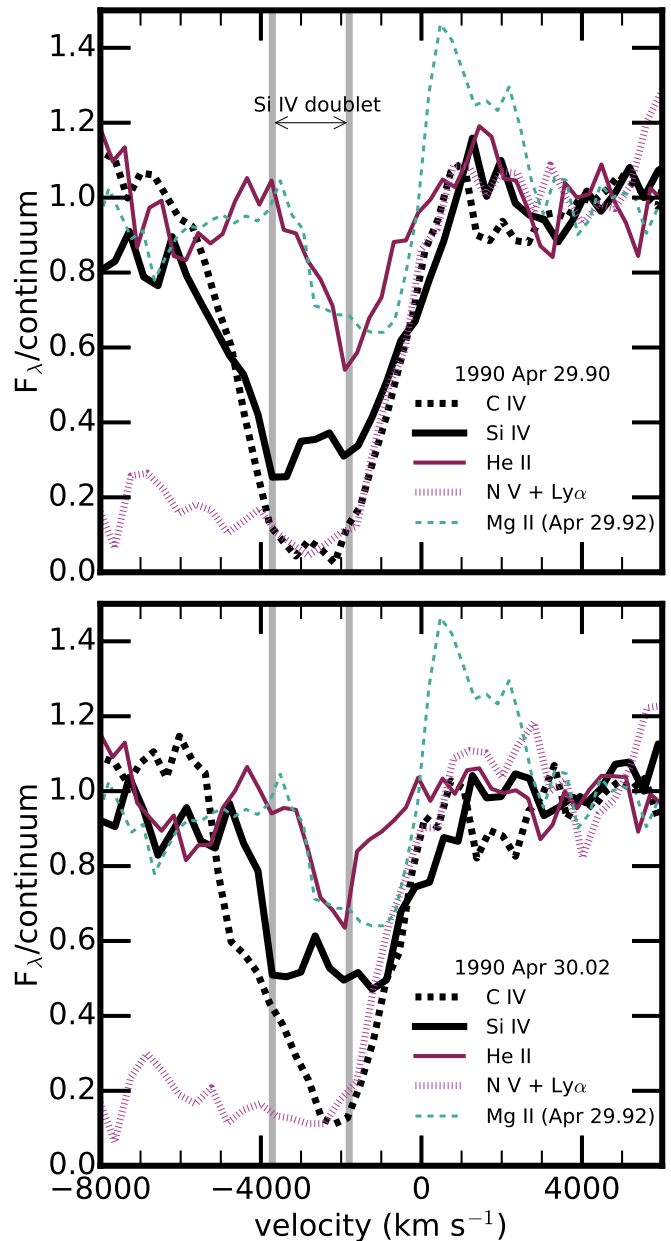


Figure 2. Velocity profiles from the high-ionization BALs in IUE spectra from 1990 April 29.90 (top) and 30.02 (bottom), and Mg II for comparison, with zero-velocity set to the rest wavelength of the reddest transition in each doublet or multiplet (§ 3.1). The Si IV doublet separation is marked at -1800 km s^{-1} . Flux density is normalized to the median value between $+3000$ and $+6000 \text{ km s}^{-1}$.

itions of blue-shifted BALs from the high-ionization C IV $\lambda 1548.20, 1550.77\text{\AA}$, Si IV $\lambda 1393.76, 1402.77\text{\AA}$, and N V $\lambda 1238.82, 1242.80\text{\AA}$ doublets and He II $\lambda 1640\text{\AA}$ multiplet, as shown by rest-wavelength line-labels in Fig. 1. The velocity profiles of these strong and rapidly variable BALs are shown in Fig. 2. The Si IV BAL is confirmed by the 9.0\AA (1900 km s^{-1}) Si IV doublet separation, which is about twice the local full-width-half-max spectral resolution and is observed in the trough (Fig. 2). Subtracting the

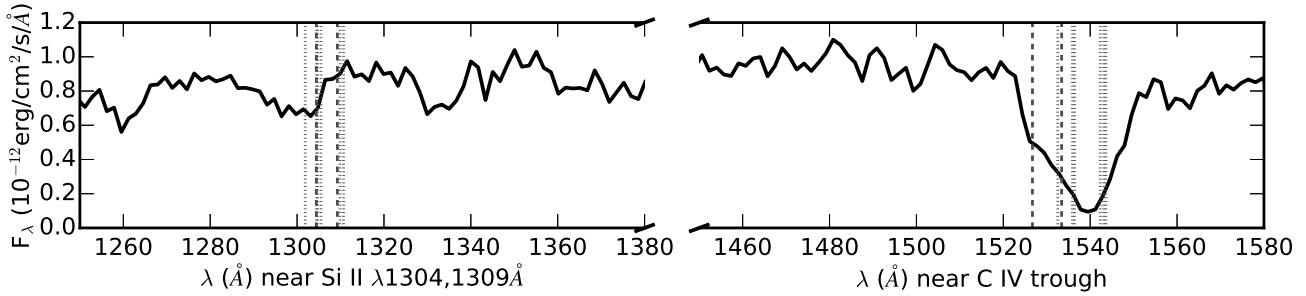


Figure 3. The vertical lines drawn on this IUE spectrum from 1990 April 30.02 are Si II (dashed) and P II (hashed) transition rest wavelengths from Table 2. Atomic physics predicts that the two absorption complexes should be comparably strong, so the comparison region (left) shows that Si II+P II cannot account for the absorption trough near 1550 Å (right).

Table 1. Selected IUE spectra of MWC 560 from Michalitsianos et al. (1991), Maran et al. (1991), and Bond et al. (1984).

Date (UT)	IUE ID	Bandpass (Å)	Resolution (Å)
1984 Mar 10.95	SWP22459	1150–1975	4–7
1984 Mar 10.93	LWP02920	1910–3300	5–8
1990 Mar 14.98	LWP17534	1910–3300	5–8
1990 Mar 14.99	SWP38361	1150–1975	4–7
1990 Apr 29.90	SWP38698	1150–1975	4–7
1990 Apr 29.92	LWP17832	1910–3300	5–8
1990 Apr 29.94	LWP17833	1845–2980	0.1–0.3
1990 Apr 30.02	SWP38699	1150–1975	4–7
1991 Sep 29.12	LWP21366	1910–3300	5–8
1991 Sep 29.14	SWP42580	1150–1975	4–7

doublet separations, the C IV and Si IV troughs extend to at least 4000 km s⁻¹. N V is contaminated by Ly α absorption at high velocities. He II extends to about 3000 km s⁻¹.

3.2 Evidence against prior identifications

The feature we assign to C IV λ 1550 Å was previously misidentified as Si II near zero-velocity (Michalitsianos et al. 1991; Maran et al. 1991) blended with P II (Maran et al. 1991). Table 2 shows that there is a complex of Si II and P II transitions near 1304 Å with lower levels and oscillator strengths almost identical to those of Si II and P II near 1550 Å. Fig. 3 shows that the 1304 Å complex is only observed weakly and at large blue-shifts (if at all) in 1990 April. Therefore, Si II and P II cannot produce the deep trough near 1550 Å. Moreover, there are no Si II transitions from close to the ground state near the feature we assign to He II λ 1640 Å, further contradicting line labels in Michalitsianos et al. (1991). Our transition data are from the National Institute of Standards and Technology (NIST; Kramida et al. 2017); we checked for additional lines in Kurucz & Bell (1995).

The lines we assign to Si IV λ 1400 Å and N V λ 1240 Å were misidentified as Fe II (Michalitsianos et al. 1991; Maran et al. 1991). In modeling the 1990 March 14 iron curtain, Shore et al. (1994) later speculated that Si IV was probably present. In fact, the situation is clearer in the 1990 April spectra, in which most Fe II absorption has vanished. Any remaining weak lines would be from easily-populated

Table 2. NIST lab data showing that the 1304 Å and 1526 Å complexes of Si II and P II share similar line strengths: wavelength (λ_{lab}), lower-level excitation above the ground state (E_l), oscillator strength (f), and lower-level statistical weight (g_l).

Ion	λ_{lab} (Å)	E_l (eV)	f	g_l
Si II	1526.71	0	0.133	2
Si II	1304.43	0	0.093	2
Si II	1533.43	0.036	0.133	4
Si II	1309.27	0.036	0.080	4
P II	1532.53	0	0.008	1
P II	1301.87	0	0.038	1
P II	1535.92	0.020	0.006	3
P II	1536.42	0.020	0.002	3
P II	1304.49	0.020	0.013	3
P II	1304.68	0.020	0.009	3
P II	1305.50	0.020	0.016	3
P II	1542.30	0.058	0.006	5
P II	1543.13	0.058	0.001	5
P II	1543.63	0.058	0.000	5
P II	1309.87	0.058	0.010	5
P II	1310.70	0.058	0.028	5

(see Lucy et al. 2014) excitations less than 0.4 eV above the ground state, there being no excitation states between 0.39 eV and 0.98 eV in the Fe⁺ atom. We summed the relative optical depths of these low-excitation lines (oscillator strength \times statistical weight \times wavelength) into 10 Å bins to show that they cannot produce deep FUV absorption without producing deep NUV absorption, which is not observed in 1990 April (Fig. 1). The only sign of iron-like absorption comes from a few of the strongest low-excitation lines (e.g., Fe II λ 2600 Å) observed in the high-resolution NUV spectrum from 1990 April 29 as zero-velocity, saturated absorption < 1 Å wide; these narrow, possibly-interstellar lines do not produce deep features in the low-resolution spectra. Thus, although low-ionization lines may weakly contaminate the high-ionization BALs on 1990 April 29–30, they cannot account for them.

4 DISCUSSION

4.1 Ionization and velocity structure

Our results show that photo-ionization is likely a prominent mechanism in the outflow from MWC 560's accretion disk. The broad and continuous velocity distributions of BALs from a wide range of ionization states argue against collisional ionization in discrete shocks or a star-like photosphere alone. Ionizing photons of at least 33, 48, and 77 eV can populate the Si IV, C IV, and N V BAL transitions, respectively; these are emitted in sufficient quantities at the $\sim 10^5$ K inner radii of a WD accretion disk with MWC 560's parameters (Schmid et al. 2001).

The presence of high-ionization lines is consistent with the high-velocity absorption from He I $\lambda 10830\text{\AA}$ in 1990 April 12 and 1991 January 25 infrared spectra of MWC 560 (Meier et al. 1996). This transition's metastable lower level is populated by recombinations of He⁺; the ionization potentials of neutral helium and He⁺ are 25 and 54 eV, respectively, so upward transitions from this state can be partially co-spatial with C IV and Si IV (Leighly et al. 2011).

The high-ionization C IV and Si IV BALs exhibit maximum radial velocities at least 1000 km s⁻¹ faster than the contemporaneous low-ionization Mg II $\lambda 2800\text{\AA}$ resonance line (Fig. 2). This behavior is also observed in BAL quasar outflows, for which various explanations have been proposed. Dense, self-shielding clumps may be embedded in a faster, higher-ionization gas (Voit et al. 1993). Equatorial winds can comprise vertically-stratified layers of ionization state and velocity (Matthews et al. 2016). Or an outflow may decelerate along the line of sight, with fast gas close to the photo-ionizing source shielding radially-slower gas closer to the observer (Voit et al. 1993). One or more of these geometries, which are not mutually-exclusive, could apply to MWC 560.

The He II BAL likewise appears to be slower than the C IV and Si IV BALs, probably for a different reason. This behavior is observed in CV and stellar winds, in which the He II $\lambda 1640\text{\AA}$ multiplet's highly-excited lower level (41 eV above the ground state) is thought to be collisionally populated in the hot, dense base of the outflow, where the gas is still accelerating (Hoare 1994; Smith 2006).

4.2 Vanishing curtains and novae

Both ground-state and high-excitation Fe⁺ vanished in 1990 April. The iron curtain has been present in every other UV spectrum of MWC 560, including observations in 1984 (Bond et al. 1984), 1990 January–March and late 1990–1993 (Michalitsianos et al. 1991; Skopal 2005), 1995 (IUE PI: Starrfield), and throughout a 2016 high state that rivaled 1990 in bolometric luminosity (Lucy et al., in preparation), suggesting that the disappearance of Fe⁺ signified more than a simple increase in ionizing luminosity.

Instead, the vanishing curtain probably corresponded to a temporary decrease in hydrogen column density—i.e., in total mass along the line of sight. In strongly photo-ionized plasma, iron is distributed between Fe⁺², Fe⁺³, and Fe⁺⁴, making it difficult to form much Fe⁺ even through recombination (see §4.3 in Lucy et al. 2014). Other 'iron curtain'

elements like silicon and chromium (but not magnesium²) have similar ionization potentials and behave in the same way. Iron curtain ions may survive only when enough mass is present to self-shield some portion of the outflow against high-energy photons.

The decline in column density during 1990 April was likely related to (1) the 1990 January–April optical brightening, which marked both a periodic peak in the system's light curve and a unique, non-periodic, and permanent tripling of the optical luminosity (Leibowitz & Formigini 2015; Munari et al. 2016); (2) the dramatic mass ejections of 1990 January–April, which yielded detached BALs blue-shifted up to a system record of 6000 km s⁻¹ (Tomov et al. 1990a, 1992); and (3) the post-outburst, year-long suppression of optical flickering and slowing of absorption speeds to less than 1000 km s⁻¹ in late 1990–1991 (Zamanov et al. 2011a). Coverage of the spectral response to these events is incomplete; to our knowledge, no optical spectra were obtained 1990 April 4 through October 22, and no UV spectra were obtained 1990 May 1 through September 25.

Although MWC 560 is unlikely to have ejected a nova-like shell³, it is nevertheless instructive to note that high-ionization UV BALs are briefly observed as P Cygni profiles immediately after an iron curtain phase in some thermonuclear novae (Shore et al. 1993; M. J. Darnley 2018, private communication). The ejected mass rarefies as it expands, erasing the outer, heretofore-shielded, Fe⁺ component. The similarity suggests that MWC 560's wind temporarily turned off in 1990 April after a series of powerful gusts, resulting in the nova-like phenomenology of a discrete mass ejection. This pattern supports the 'discrete' and 'quasi-stationary' taxonomy proposed by Kolev & Tomov (1993) for MWC 560's optical absorption lines.

4.3 A BAL nano-quasar

To our knowledge, there is no other accretion disk in the Galaxy observed to contain a similar range of ionization and excitation states in a persistent BAL outflow. There are CVs that exhibit both Balmer and C IV BALs (Kafka & Honeycutt 2004), but we have found no reports of any CV or X-ray binary known to have *also* exhibited Mg II and Fe II BALs except during thermonuclear novae. Unlike novae, Balmer BALs and the iron curtain are almost-permanent properties of MWC 560's spectrum for years at a time. Likewise, the high-ionization UV BALs may be present in every MAST-archived FUV spectrum of MWC 560, including the one obtained by Bond et al. (1984), although contamination by the optically thick iron curtain precludes certainty at all epochs besides 1990 April.

Rather, MWC 560 best resembles Balmer FeLoBAL

² Although Mg⁺ and Fe⁺ have similarly small ionization potentials, Mg⁺² can dominate thanks to its large 80 eV ionization potential; recombination can then yield sufficient Mg⁺ for opacity at 2800Å (Lucy et al. 2014), explaining the persistence of that BAL in MWC 560.

³ The optical photometry did not appear to fade substantially during 1990 April–May (Tomov et al. 1990b), in contrast to the optical decline observed during the lifting of the iron curtain in novae (e.g., Shore 2012).

quasars, wherein photo-ionization models favor high densities in the BAL wind—comparable to densities in symbiotic nebulae (§ 1). These quasar winds persistently exhibit a similarly wide range of ionization states⁴ and similar spectra; see the quasar spectra in Fig. 1. Moreover, iron curtain absorption has recently been observed to vary dramatically and even vanish in some FeLoBAL quasars, albeit on slower timescales than in MWC 560 (Rafee et al. 2016; see also Hall et al. 2011; McGraw et al. 2015; Zhang et al. 2015; Stern et al. 2017).

4.4 The BAL symbiotics

The C IV, Si IV, and N V BALs in MWC 560 illuminate a link to another symbiotic WD+RG binary: Munari & Buson (1993) showed that AS 304 contains absorption blue-shifted up to $2200 \pm 400 \text{ km s}^{-1}$ from *only* C IV, Si IV, and N V. Its FUV spectrum was observed only in 1992, but this observation was not prompted by any particular event, so there is no reason to think that the BALs were transient. The He II emission strength indicated a high luminosity on the order of $10^4 L_{\odot}$ (Munari & Buson 1993), which likely required nuclear burning on the surface of the white dwarf to power. The ionization parameter in AS 304’s outflow was therefore large, contributing to the absence of low-ionization (and in this case, optical) absorption.

In MWC 560, optical and UV flickering (Bond et al. 1984; Tomov et al. 1996; Zamanov et al. 2011b; Lucy et al., in preparation; though see Zamanov et al. 2011a) and hard X-rays sometimes observed from the boundary layer (Stute & Sahai 2009) indicate an accretion disk without WD surface burning (see Luna et al. 2013). Thus, both hot burning (AS 304) and cooler non-burning (MWC 560) symbiotics can sustain persistent BAL outflows.

MWC 560 and AS 304 have cousins in symbiotics with transient or low-velocity absorption. CH Cyg, a non-burning WD+RG binary with optical flickering, exhibited Balmer BALs with blue edges around 2000 km s^{-1} in 2017 January (Iijima 2017); this absorption recurred sporadically throughout the year (Teyssier & et al. 2017), sometimes appearing and vanishing within 1.5 hours (T. Iijima 2017, private communication). Z And, a burning-powered WD+RG binary, briefly exhibited a Balmer BAL blue-shifted up to $\approx 1700 \text{ km s}^{-1}$ on 2006 July 9 (Figure 7 in Tomov et al. 2013), near the peak of a 2 magnitude optical outburst. Meanwhile, many more symbiotics (Tomov et al. 2013) and purported Be stars with cool giant companions (including the iron stars; Cool et al. 2005) exhibit substantially narrower 100–1000 km s^{-1} absorption lines; we will not here attempt to disentangle their heterogeneous population, but some may mimic BAL outflow behaviors (Tomov et al. 2013).

The transient BAL outflows from symbiotics coexist with narrow jets, but the lines of sight to Z And and CH Cyg are severely misaligned from any plausible jet axis. Eclipses in CH Cyg indicate a large inclination angle (Skopal et al. 1996) and the jet is extended in the plane of the sky (Weston 2016, and references therein), suggesting that the jet cannot

produce the BALs. We view Z And’s orbit at an inclination angle of $47 \pm 12^{\circ}$ (Schmid & Schild 1997), and marginally resolved jets have been seen perpendicular to the orbital plane (Brocksopp et al. 2004) and 20° west of the perpendicular’s projection in the sky (Sokoloski et al. 2006; Kenny 1995). Burmeister & Leedj arv (2007) inferred a 1700 km s^{-1} jet during the 2006 outburst from narrow emission lines at $\pm 1150 \text{ km s}^{-1}$, assuming that the jet was perpendicular to the orbit. Speculatively, the similarity between the jet and BAL velocity during this outburst might suggest that the opening angle of a jet-feeding wind briefly spread into the line of sight.

Likewise, the degree to which MWC 560’s outflow is collimated could vary with its strength. It probably is a generally polar outflow viewed at a small inclination angle⁵, but BAL quasars and CV winds show that it is problematic to constrain the degree to which a BAL outflow is collimated just from the ratio of absorption to emission equivalent widths (Turnshek 1997; Hamann et al. 1993; Voit et al. 1993; Drew 1987). BAL-producing outflows with wider opening angles than jets would help to explain the high incidence rate of BAL symbiotics, which now appear to be surprisingly well represented among the ~ 10 (e.g., Brocksopp et al. 2004) symbiotics with known jets. Even with large half-opening angles up to $\pm 15^{\circ}$ (as for the R Aqr jet; Schmid et al. 2017), less than 3.5% of jets should point towards Earth—although a larger fraction might exhibit slower and shallower absorption projected into the line of sight.

Voit et al. (1993) proposed that low-ionization BAL quasars (cf. MWC 560, Z And in outburst, and CH Cyg) may represent a young evolutionary phase when accretion disk outflows entrain an ambient shroud of dust and gas, which disperses to lower column densities once exclusively high-ionization BALs are observed (cf. AS 304). The dense, frequently Fe⁺-rich nebulae from cool-giant mass loss in symbiotic binaries (Shore & Aufdenberg 1993) resemble young quasar environments. We predict that higher-cadence FUV/optical spectral observations and larger sample sizes of both burning and non-burning symbiotics will lead to the detection of more BAL systems than narrow jets alone could produce, and open a window into the physics and geometry of quasar outflows on a nano-scale.

5 CONCLUSIONS

- A. The FUV spectrum of symbiotic star MWC 560 contains high-ionization BALs from C IV, Si IV, N V, and He II (§ 3, Fig. 2). They were unveiled most clearly on 1990 April 29–30, the only time throughout decades of UV observations that MWC 560’s curtain of low-ionization iron absorption vanished (Fig. 1).
- B. The maximum radial velocities of the Mg II and He II BALs were at least 1000 km s^{-1} slower than contemporaneous C IV and Si IV BALs. These differences have precedents; Mg II is slower than C IV and Si IV in BAL quasars, and He II is slower than C IV and Si IV in CV and stellar winds (§ 4.1).

⁴ Except for He II, whose absence in quasar outflows has been interpreted as a lower limit on the distance of absorbing material from the disk (Wampler et al. 1995).

⁵ See discussion in Schmid et al. (2001) of unpublished echelle-spectrograph limits on TiO absorption band motion.

- C. The usually-persistent wind in MWC 560 temporarily switched to a discrete ejection phase in 1990. This finding is supported by the phenomenology of some novae, in which the iron curtain lifts to unveil high-ionization UV BALs (§ 4.2).
- D. Additional BAL symbiotics exist (§ 4.4). The high-ionization BALs in MWC 560 illustrate a similarity to symbiotic star AS 304, which exhibits exclusively C IV, Si IV, and N V BALs (Munari & Buson 1993). Z And and CH Cyg have exhibited transient Balmer BALs (Tomov et al. 2013; Iijima 2017); these transient BAL symbiotics contain jets, but the jets do not point towards Earth. Wide-angle disk winds are sometimes required to explain the BAL symbiotics, and may account for why the number of symbiotics with BALs is no longer negligible relative to the ~ 10 symbiotics with jets.
- E. MWC 560 and AS 304 most resemble Balmer FeLoBAL quasars and high-ionization BAL quasars, respectively (§ 4.3, § 4.4). Both symbiotic star and quasar accretion disks are sometimes embedded in regions of dense gas and dust, so the evolution of these systems may involve similar physics.

ACKNOWLEDGEMENTS

We thank Matt Darnley for insights on connections to novae and editorial comments. ABL thanks Ulisse Munari, Karen Leighly, and Takashi Iijima for other edifying conversations. We thank Michael Rupen, Paul Kuin, Nirupam Roy, Gerardo Juan Manuel Luna, Jennifer Weston, and Peter Somogyi for editorial comments. ABL thanks the LSSTC Data Science Fellowship Program; their time as a Fellow has benefited this work. We are supported by NSF DGE-16-44869 (ABL), NSF AST-1616646 (JLS), and *Chandra* DD6-17080X (ABL, JLS). We gratefully acknowledge our use of pysynphot (STScI Development Team 2013), PyAstronomy (<https://github.com/sczesla/PyAstronomy>), extinction (Barbary 2016), the Mikulski Archive for Space Telescopes (MAST), the International Ultraviolet Explorer (IUE), the Sloan Digital Sky Survey (SDSS), NASA's Astrophysics Data System (ADS), the SIMBAD database operated at CDS, and the National Institute of Standards and Technology (NIST).

References

- Barbary K., 2016, extinction v0.3.0, doi:10.5281/zenodo.804967, [extinction.readthedocs.io](https://github.com/abl/ablib)
- Bond H. E., Pier J., Pilachowski C., Slovak M., Szkody P., 1984, in *Bulletin of the American Astronomical Society*. p. 516
- Brocksopp C., Sokolowski J. L., Kaiser C., Richards A. M., Muxlow T. W. B., Seymour N., 2004, *MNRAS*, **347**, 430
- Burmeister M., Leedj arv L., 2007, *A&A*, **461**, L5
- Cool R. J., Howell S. B., Pe a M., Adamson A. J., Thompson R. R., 2005, *PASP*, **117**, 462
- Drew J. E., 1987, *MNRAS*, **224**, 595
- Gibson R. R., et al., 2009, *ApJ*, **692**, 758
- Gordon K. D., Clayton G. C., Misselt K. A., Landolt A. U., Wolff M. J., 2003, *ApJ*, **594**, 279
- Green G. M., et al., 2015, *ApJ*, **810**, 25
- Hall P. B., 2007, *AJ*, **133**, 1271
- Hall P. B., et al., 2002, *ApJS*, **141**, 267
- Hall P. B., Anosov K., White R. L., Brandt W. N., Gregg M. D., Gibson R. R., Becker R. H., Schneider D. P., 2011, *MNRAS*, **411**, 2653
- Hamann F., Korista K. T., Morris S. L., 1993, *ApJ*, **415**, 541
- Hoare M. G., 1994, *MNRAS*, **267**, 153
- Iijima T., 2017, *The Astronomer's Telegram*, **10142**
- Kafka S., Honeycutt R. K., 2004, *AJ*, **128**, 2420
- Kenny H. T., 1995, PhD thesis, University of Calgary (Canada)
- Knigge C., Scaringi S., Goad M. R., Cottis C. E., 2008, *MNRAS*, **386**, 1426
- Kolev D., Tomov T., 1993, *A&AS*, **100**, 1
- Kramida A., Ralchenko Y., Reader J., and NIST ASD Team 2017, NIST Atomic Spectra Database (ver. 5.5.5), [Online]. Available: <https://physics.nist.gov/asd> [2017 November]. National Institute of Standards and Technology, Gaithersburg, MD.
- Kurucz R. L., Bell B., 1995, Atomic Line Data, Kurucz CD-ROM No. 23, Cambridge, Mass.: Smithsonian Astrophysical Observatory, <https://www.cfa.harvard.edu/amp/ampdata/kurucz23/sekur.html>
- Leibowitz E. M., Formiggin L., 2015, *AJ*, **150**, 52
- Leighly K. M., Dietrich M., Barber S., 2011, *ApJ*, **728**, 94
- Lucy A. B., Leighly K. M., Terndrup D. M., Dietrich M., Gallagher S. C., 2014, *ApJ*, **783**, 58
- Luna G. J. M., Sokolowski J. L., Mukai K., Nelson T., 2013, *A&A*, **559**, A6
- Maran S. P., Michalitsianos A. G., Oliverson R. J., Sonneborn G., 1991, *Nature*, **350**, 404
- Matthews J. H., Knigge C., Long K. S., Sim S. A., Higginbottom N., Mangham S. W., 2016, *MNRAS*, **458**, 293
- McGraw S. M., Shields J. C., Hamann F. W., Capellupo D. M., Gallagher S. C., Brandt W. N., 2015, *MNRAS*, **453**, 1379
- Meier S. R., Rudy R. J., Lynch D. K., Rossano G. S., Erwin P., Puetter R. C., 1996, *AJ*, **111**, 476
- Michalitsianos A. G., Maran S. P., Oliverson R. J., Bopp B., Kontizas E., Dapergolas A., Kontizas M., 1991, *ApJ*, **371**, 761
- Munari U., Buson L. M., 1993, *MNRAS*, **263**, 267
- Munari U., et al., 2016, *New Astron.*, **49**, 43
- Rafiee A., Pirkola P., Hall P. B., Galati N., Rogerson J., Ameri A., 2016, *MNRAS*, **459**, 2472
- STScI Development Team 2013, pysynphot: Synthetic photometry software package, Astrophysics Source Code Library (ascl:1303.023)
- Schmid H. M., Schild H., 1997, *A&A*, **327**, 219
- Schmid H. M., Kaufer A., Camenzind M., Rivinius T., Stahl O., Szeifert T., Tubbesing S., Wolf B., 2001, *A&A*, **377**, 206
- Schmid H. M., et al., 2017, *A&A*, **602**, A53
- Shlosman I., Vitello P., 1993, *ApJ*, **409**, 372
- Shore S. N., 2012, *Bulletin of the Astronomical Society of India*, **40**, 185
- Shore S. N., Aufdenberg J. P., 1993, *ApJ*, **416**, 355
- Shore S. N., Sonneborn G., Starrfield S., Riestra-Gonzalez R., Ake T. B., 1993, *AJ*, **106**, 2408
- Shore S. N., Aufdenberg J. P., Michalitsianos A. G., 1994, *AJ*, **108**, 671
- Skopal A., 2005, *A&A*, **440**, 995
- Skopal A., Bode M. F., Lloyd H. M., Tamura S., 1996, *A&A*, **308**, L9
- Smith M. A., 2006, *A&A*, **459**, 215
- Sokolowski J. L., et al., 2006, *ApJ*, **636**, 1002
- Stern D., et al., 2017, *ApJ*, **839**, 106
- Stute M., Sahai R., 2009, *A&A*, **498**, 209
- Teyssier F., et al., 2017, ARAS Eruptive Stars Information Letter, n^o 36, http://www.astrosurf.com/aras/novae/InformationLetter/ARAS_EruptiveStarsInfoLetter/ARAS_EruptiveStarsInfoLetter_n36.pdf
- Tomov T., Kolev D., Georgiev L., Zamanov R., Antov A., Bellas Y., 1990a, *Nature*, **346**, 637

- Tomov T., Zamanov R., Antov A., Georgiev L., 1990b, *Information Bulletin on Variable Stars*, [3466](#)
- Tomov T., Zamanov R., Kolev D., Georgiev L., Antov A., Mikolajewski M., Esipov V., 1992, *MNRAS*, [258](#), [23](#)
- Tomov T., et al., 1996, *A&AS*, [116](#), [1](#)
- Tomov N. A., Tomova M. T., Bisikalo D. V., 2013, in Zhelyazkov I., Mishonov T. M., eds, *American Institute of Physics Conference Series Vol. 1551*, American Institute of Physics Conference Series. pp 30–45 ([arXiv:1301.2762](#)), [doi:10.1063/1.4818851](#)
- Turnshek D. A., 1997, in Arav N., Shlosman I., Weymann R. J., eds, *Astronomical Society of the Pacific Conference Series Vol. 128*, *Mass Ejection from Active Galactic Nuclei*. p. 52
- Voit G. M., Weymann R. J., Korista K. T., 1993, *ApJ*, [413](#), [95](#)
- Wampler E. J., Chugai N. N., Petitjean P., 1995, *ApJ*, [443](#), [586](#)
- Weston J. H. S., 2016, PhD thesis, Columbia University, [doi:10.7916/D87M082M](#)
- Weymann R. J., Morris S. L., Foltz C. B., Hewett P. C., 1991, *ApJ*, [373](#), [23](#)
- Williams R. J., Maiolino R., Krongold Y., Carniani S., Cresci G., Mannucci F., Marconi A., 2017, *MNRAS*, [467](#), [3399](#)
- Zamanov R., Marziani P., 2002, *ApJ*, [571](#), [L77](#)
- Zamanov R. K., Tomov T., Bode M. F., Mikolajewski M., Stoyanov K. A., Stanishev V., 2011a, *Bulgarian Astronomical Journal*, [16](#), [3](#)
- Zamanov R., Boeva S., Latev G., Stoyanov K., Bode M. F., Antov A., Bachev R., 2011b, *Information Bulletin on Variable Stars*, [5995](#)
- Zhang S., et al., 2015, *ApJ*, [803](#), [58](#)

This paper has been typeset from a $\text{\TeX}/\text{\LaTeX}$ file prepared by the author.